GNSS-antenna lever arm compensation in aided inertial navigation of UAVs

Bård N. Stovner* and Tor A. Johansen*

***Abstract*— This paper considers aided inertial navigation of unmanned aerial vehicles aided with position measurements from one or more global navigation satellite system antennas, where the exact positions of the antennas are assumed unknown. This reflects that the antennas' location relative to the inertial sensor, i.e. the lever arms, might be difficult to measure accurately in the coordinate frame of the inertial sensor. Using inaccurate lever arm values will deteriorate both the position and attitude estimates of the vehicle. It is easier to manually and accurately measure the distances from each antenna to the inertial sensor and between antennas, and this information can be used constructively to estimate the lever arms online. In this paper, the distance information is used to reduce the representation of one or more lever arms to two or three states, respectively. An error-state extended Kalman filter is derived and compared to two other similar filters in simulations: one filter in which the lever arms are known and one which represents all lever arms as body-fixed positions. The suggested filter is shown to perform as well as the latter, but with a significantly smaller state space representation.**

I. INTRODUCTION

Navigation of unmanned aerial vehicles (UAVs) usually involves the fusion of global navigation satellite system (GNSS) and inertial measurement unit (IMU) measurements, i.e, from an accelerometer and angular rate sensor (ARS). The accuracy of estimation depends largely on the magnitude of sensor noise and the calibration of the sensors. Calibration relates to biases, misalignments, and scale factors in the accelerometer and ARS that causes estimates to drift; lever arm from center of gravity (CG) to the IMU that produces centrifugal accelerations; and lever arm from the IMU to GNSS antennas. The misalignments and scale factors of the IMU are often calibrated pre-flight, while biases are often estimated online. The lever arm from CG to the IMU can often be made small and therefore negligible. For position estimation, failing to compensate for the lever arm from the IMU to the GNSS antennas yields an attitude dependent error. In the case of multiple GNSS antennas on the UAV, position measurements will give valuable attitude information which further necessitates precise knowledge of the GNSS antennas' body-fixed position. If GNSS velocity measurements are used, angular rates will give an additional velocity term proportional to the length of the lever arm, which is important to account for.

The lever arms, from now on meaning the GNSS antennas' position relative to the IMU, are hard to measure accurately in the IMU's coordinate frame, and an offline calibration or online estimation scheme is therefore useful. Hong et al. [1] analytically examined the observability of the position, velocity, attitude, accelerometer and ARS biases, and the lever arm of a single GNSS antenna, where the lever arm was represented as a three-parameter position vector. Hong et al. [2] conducted an experimental analysis on the same problem. Lee et al. [3] and Hong et al. [4] examined the observability of the same problem with multiple GNSS antennas analytically and with experiments, respectively. There, a minimum of three antennas were required. One of the antennas was defined as the origin of an antenna coordinate frame in which the positions of the other antennas are measured. This resulted in all the lever arms being represented by six variables: three translations and three rotations from the body-fixed frame to the antenna coordinate frame. It was found that angular velocity was required to observe the lever arms both with a single and two GNSS antennas. For one antenna, the angular velocity about an axis only helped in observing the components of the lever arms off, but not along, the axis of rotation. Therefore, the axis of rotation needs to change over time.

In Seo et al. [5], a GNSS lever arm is estimated in integration with IMU and odometer measuring the distance traveled in a car wheel. Zhong et al. [6] and Cao, Zhong, and Zhao [7] considers estimation of a dynamic lever arm between a GNSS antenna and an IMU on a gimballed platform also carrying an optical sensor. Estimation of the spatial relationship between sensors is often encountered in systems with IMUs and cameras. This entails estimation of three translations and three rotations in the general case, similarly as in the multiple GNSS antenna case in Lee et al. [3] and Hong et al. [4]. Examples of this include Chiang et al. [8] and Lobo and Dias [9]. Montalbano and Humphreys [10] compared lever-arm compensation by an extended Kalman filter (EKF) to multiple-model Kalman filters and a neural network, finding that the EKF outperformed the other methods. Wu, Wang, and Hu [11] posed the estimation of attitude, acceleration and ARS biases, and GNSS lever arm as an optimization problem and solved it using a recursive Lagrange-Newton method.

It is not straightforward to measure the lever arms manually since the IMU's coordinate frame is not known exactly. However, the lengths of the lever arms are often straightforward to manually measure with high accuracy. This is also true for the distances between antennas. This motivates the development of a lever arm formulation using the known distances to yield a minimal lever arm representation. Inspired by Lee et al. [3] and Hong et al. [4], an antenna coordinate

*Center for Autonomous Marine Operations and Systems (NTNU-AMOS), Department of Engineering Cybernetics, Norwegian University of Science and Technology, Trondheim, Norway

frame is found, in which the GNSS antennas positions are known. In this paper, however, the IMU is used as the origin of the antenna coordinate frame. This relieves the need for estimating a translation between the IMU and the antenna frame, since the origins coincide. Also, only two antennas are now required to define the antenna frame. This means that for two or more antennas, the lever arms can be represented by three rotations only.

Aided inertial navigation of UAVs without the lever arm compensation is a thoroughly studied field of which there exists a multitude of estimators, e.g., EKFs, see Farrell [12] and George and Sukkarieh [13], and nonlinear observers, see Vik and Fossen [14], Hua [15], Grip et al. [16], and Hansen, Johansen, and Fossen [17]. In this paper, the position, velocity, attitude, ARS and accelerometer biases, and lever arm are estimated by an error-state EKF. The lever arm representations for a single and multiple GNSS antennas are developed in Section III, before the error-state EKF is derived in Section IV. It is shown that the EKF using the novel minimal representation of the lever arm performs equally well, and with a smaller state space representation than, the EKF in which lever arms are represented as three-parameter positions and the measured distances are used as pseudo-measurements.

II. PRELIMINARIES AND MODELS

A. Notation

Denote by x^a_{bc} the position, velocity, or acceleration x of point c relative to point b decomposed in the coordinate frame $\{a\}$. In the case of angular velocity, ω^a_{bc} denotes angular rate of the coordinate frame $\{c\}$ relative to coordinate frame $\{b\}$ decomposed in the coordinate frame $\{a\}$. Let R^d_e denote the rotation matrix expressing the rotation from coordinate frame $\{e\}$ to coordinate frame $\{d\}$.

3×3 and 4×4 skew-symmetric matrices are useful to define for any vector $\omega = [\omega_1, \omega_2, \omega_3]^\top$

$$S(\omega) \triangleq \begin{bmatrix} 0 & -\omega_3 & \omega_2 \\ \omega_3 & 0 & -\omega_1 \\ -\omega_2 & \omega_1 & 0 \end{bmatrix} \Omega(\omega) \triangleq \begin{bmatrix} 0 & -\omega^\top \\ \omega & -S(\omega) \end{bmatrix}$$

A stochastic variable $\epsilon \in \mathbb{R}^N$ that is Gaussian with mean $m \in \mathbb{R}^N$ and covariance $C \in \mathbb{R}^{N \times N}$ is denoted $\epsilon \sim \mathcal{N}(m, C)$.

0_3 and I_3 denote 3×3 zero and identity matrices, respectively.

B. Representations of Rotation

Rotations are in this paper either represented by the quaternion $q^d_e = [\eta^d_e, \varepsilon^{d\top}_e]^\top$, the rotation matrix $R^d_e = R(q^d_e)$, or by four times the modified Rodrigues parameter (MRP) $u^d_e = u(q^d_e)$, where

$$R(q^d_e) = I_3 + 2\eta^d_e S(\varepsilon^d_e) + 2S(\varepsilon^d_e)^2 \tag{1}$$

$$u(q^d_e) = 4\frac{\varepsilon^d_e}{1+\eta^d_e} \tag{2}$$

The quaternion is found from the MRP by

$$q(u^d_e) = \frac{1}{16 + \|u^d_e\|_2^2} \begin{bmatrix} 16 - \|u^d_e\|_2^2 \\ 8u^d_e \end{bmatrix} \tag{3}$$

The attitude error in the EKF's error state is best represented by a three-parameter variable. The choice of attitude error representation falls on the MRP due to its less inhibiting singularity at 360° compared to the Gibbs vector's 180° and the Euler angle's 90°, Markley and Crassidis [18]. The MRP is scaled with a factor of four in order to be able to use the results in Markley [19].

C. States and Coordinate Frames

The north-east-down (NED) coordinate frame $\{n\}$ is a local tangent frame which is used as the global reference frame in this paper, while the body-fixed frame $\{b\}$ is defined as the IMU's coordinate frame. For two or more GNSS antennas, the antenna frame $\{a\}$ is defined. The estimated body-fixed and antenna frames are denoted $\{\hat{b}\}$ and $\{\hat{a}\}$, respectively.

The states that are estimated by the EKF are the position of the UAV in the NED frame, p^n_{nb}, the velocity v^n_{nb}, accelerometer bias b^b_{acc}, attitude q^n_b, ARS bias b^b_{ars}, and the lever arm angles q^b_a in the case of multiple antennas or the inclination and azimuth angles ζ and ξ, respectively, in the case of one antenna, see Figure 1.

D. Measurements

1) GNSS Position Measurements: The GNSS position measurement of GNSS antenna i provides position measurements

$$p^n_{na_i,m} = p^n_{nb} + R^n_b p^b_{ba_i} + \epsilon_{p,i} \tag{4}$$

where $p^b_{ba_i}$ denotes the position of antenna i relative to the body-fixed frame decomposed in the body-fixed frame and $\epsilon_{p,i} \in \mathcal{N}(0, \mathcal{R}_i)$. It is emphasized that $p^b_{ba_i}$ is not known. Its representation is covered in detail in Section III.

2) IMU Measurements: The IMU contains a 3-axis accelerometer and an ARS that measure

$$f^b_{nb,m} = R^{n\top}_b (a^n_{nb} - g^n) + b^b_{acc} + \epsilon_{acc} \tag{5a}$$

$$\omega^b_{nb,m} = \omega^b_{nb} + b^b_{ars} + \epsilon_{ars} \tag{5b}$$

respectively, where a^n_{nb} is the acceleration of the vehicle, $g^n = [0, 0, 9.81]^\top$ is the acceleration of gravity, b^b_{acc} and b^b_{ars} are bias terms that are assumed to be constant or slowly varying, i.e.

$$\dot{b}^b_{acc} = \epsilon_{b_{acc}} \tag{6}$$

$$\dot{b}^b_{ars} = \epsilon_{b_{ars}} \tag{7}$$

and

$$\epsilon_{acc} \sim \mathcal{N}(0, Q_{acc}), \ \epsilon_{ars} \sim \mathcal{N}(0, Q_{ars}) \tag{8}$$

$$\epsilon_{b_{acc}} \sim \mathcal{N}(0, Q_{b_{acc}}), \ \epsilon_{b_{ars}} \sim \mathcal{N}(0, Q_{b_{ars}}) \tag{9}$$

Note that (5b) does not include Earth's rotation, implicitly assuming that NED is inertial.

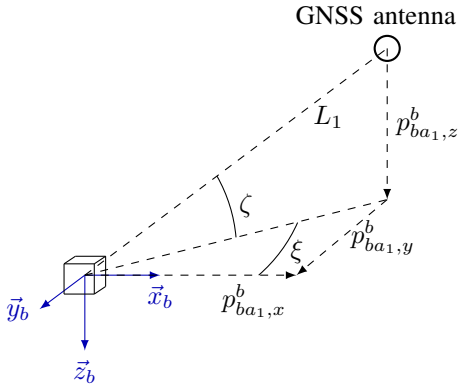

Fig. 1: This figure shows the IMU (box), its body-fixed frame $\{b\}$ (blue), and how the inclination and azimuth angles ζ and ξ, respectively, are defined in the case of one GNSS antenna.

E. Kinematics

The kinematics of position, velocity, and attitude are

$$\dot{p}^n_{nb} = v^n_{nb} \tag{10}$$
$$\dot{v}^n_{nb} = a^n_{nb} = R^n_b(f^b_{nb,m} - b^b_{acc} - \epsilon_{acc}) + g^n \tag{11}$$
$$\dot{q}^n_b = \frac{1}{2}\Omega(\omega^b_{nb})q^n_b = \frac{1}{2}\Omega(\omega^b_{nb,m} - b^b_{ars} - \epsilon_{ars})q^n_b \tag{12}$$

III. Lever-arm representations

Assume that the aircraft is equipped with M GNSS antennas whose distance to the IMU and each other are measured accurately. Denote by $L_i = \|p^b_{ba_i}\|_2$ the distance between antenna i and the IMU and by $L_{ij} = \|p^b_{ba_i} - p^b_{ba_j}\|_2$ the distance between antennas i and j, where $i, j \in (1, M)$.

A. One antenna

Spherical coordinates represents a point in space by the distance to that point and by inclination and azimuth angles. Since the distance between the IMU and the single antenna on the UAV is assumed to be measured accurately, using spherical coordinates to represent its position reduces the state space dimension by one, i.e.

$$p^b_{ba_1} = \begin{bmatrix} L_1\cos(\zeta)\cos(\xi) \\ L_1\cos(\zeta)\sin(\xi) \\ -L_1\sin(\zeta) \end{bmatrix} \tag{13}$$

where L_1 is known and ζ and ξ are the inclination and azimuth angles, respectively. The spherical representation of the lever arm is shown in Figure 1. The unknown inclination and azimuth angles are assumed to be constant, i.e.

$$\dot{\zeta} = 0 \tag{14}$$
$$\dot{\xi} = 0 \tag{15}$$

B. Multiple antennas

For multiple antennas, the idea is to define a common GNSS antenna coordinate frame, denoted $\{a\}$, in which the position of all GNSS antennas are described. The origin of the antenna frame coincides with the origin of the body-fixed frame, and rotation from the antenna frame to the body-fixed frame is the goal of estimation. By doing this, we utilize the information we can know with relatively high accuracy, i.e. the distances between sensors, while reducing the state space augmentation to three variables for an arbitrary number of antennas $M \geq 2$.

Figure 2 shows how the antenna frame is defined and its relationship with the body-fixed frame. The x-axis of the antenna-frame is defined to point from the IMU towards antenna 1, meaning that it must take the form $p^a_{ba_1} \triangleq [x_1, 0, 0]^\top$. Furthermore, it is obvious that $x_1 \equiv L_1$. The y-axis is now defined by the perpendicular projection of the vector from the IMU to antenna 2 onto the x-axis. Thus, the position of the second antenna takes the form $p^a_{ba_2} \triangleq [x_2, y_2, 0]^\top$. Pythagorean trigonometry now reveals

$$L_2^2 = x_2^2 + y_2^2,\ L_{12}^2 = (L_1 - x_2)^2 + y_2^2 \tag{16}$$
$$L_{12}^2 = L_1^2 - 2L_1x_2 + x_2^2 + y_2^2 = L_1^2 - 2L_1x_2 + L_2^2 \tag{17}$$
$$x_2 = \frac{L_1^2 + L_2^2 - L_{12}^2}{2L_1},\ y_2 = \sqrt{L_2^2 - x_2^2} \tag{18}$$

Having defined the x- and y-axes, the z-axis is defined to make a right-handed coordinate system.

For any antenna $i \geq 3$, $p^a_{ba_i} = [x_i, y_i, z_i]^\top$ can be calculated explicitly or found by formulating a least squares optimization problem. The explicit calculations of x_i, y_i, and z_i for $i \geq 3$ follows4. Firstly, x_i can be calculated by

$$L_{1i}^2 - L_1^2 - L_i^2 = -2{p^a_{ba_1}}^\top p^a_{ba_i} = -2x_1x_i$$
$$x_i = \frac{L_1^2 + L_i^2 - L_{1i}^2}{2x_1} \tag{19}$$

Secondly, y_i is calculated in a similar fashion:

$$L_{2i}^2 - L_2^2 - L_i^2 = -2{p^a_{ba_2}}^\top p^a_{ba_i} = -2(x_2x_i + y_2y_i) \tag{20}$$
$$y_i = \frac{L_2^2 + L_i^2 - L_{2i}^2 - x_2x_i}{2y_2} \tag{21}$$

Finally, z_i is calculated by

$$z_i = s_i\sqrt{L_3^2 - x_i^2 - z_i^2} \tag{22}$$

where s_i contains the sign, i.e., whether $p^a_{ba_i}$ lies on the positive or negative side of the x-y-plane of the antenna frame. The sign parameters s_i has to be input manually. The GNSS lever-arms are now expressed as $p^b_{ba_i} = R(q^b_a)p^a_{ba_i}$. Since the antennas are assumed to be fixed in the body-fixed frame, we have that

$$\dot{q}^b_a = 0 \tag{23}$$

The rotation from $\{a\}$ to $\{b\}$ represented by q^b_a is now the only unknown lever arm parameter.

IV. The Error-State EKF

In this section, the estimator is derived, which is an error-state EKF.

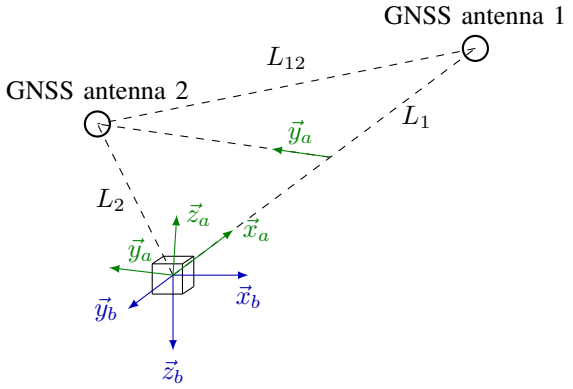

Fig. 2: This figure shows the IMU (box), its body-fixed frame $\{b\}$ (blue), and how the antenna frame $\{a\}$ (green) is defined in the presence of multiple antennas.

A. Error Kinematics Model

The error-state EKF updates the estimates of position $\hat{p}^n_{nb}$, velocity $\hat{v}^n_{nb}$, acceleration bias $\hat{b}^{\hat{b}}_{acc}$, attitude $q^n_{\hat{b}}$, ARS bias $\hat{b}^{\hat{b}}_{ars}$, and the rotation from the body-fixed frame to the antenna frame $q^b_{\hat{a}}$. The vector of estimates is denoted

$$\hat{x} = \begin{bmatrix} \hat{p}^n_{nb} \\ \hat{v}^n_{nb} \\ \hat{b}^{\hat{b}}_{acc} \\ q^n_{\hat{b}} \\ \hat{b}^{\hat{b}}_{ars} \\ q^b_{\hat{a}} \end{bmatrix}$$

The estimates are propagated according to

$$\dot{\hat{p}}^n_{nb} = \hat{v}^n_{nb} \tag{24}$$
$$\dot{\hat{v}}^n_{nb} = R^n_{\hat{b}}(f^b_{nb,m} - \hat{b}^{\hat{b}}_{acc}) + g^n \tag{25}$$
$$\dot{\hat{b}}^{\hat{b}}_{acc} = 0 \tag{26}$$
$$\dot{q}^n_{\hat{b}} = \frac{1}{2}\Omega(\omega^b_{nb,m} - \hat{b}^{\hat{b}}_{ars})q^n_{\hat{b}} \tag{27}$$
$$\dot{\hat{b}}^{\hat{b}}_{ars} = 0 \tag{28}$$

along with

$$\dot{\hat{\zeta}} = 0 \tag{29}$$
$$\dot{\hat{\xi}} = 0 \tag{30}$$

for one antenna and

$$\dot{q}^b_{\hat{a}} = 0 \tag{31}$$

for multiple antennas.

The attitude error estimates are represented by four times the MRPs, which is computed from the quaternion by (2). Now, we are ready to define the error-states

$$\delta p \triangleq p^n_{nb} - \hat{p}^n_{nb},\ \delta v \triangleq v^n_{nb} - \hat{v}^n_{nb} \tag{32}$$
$$\delta b_{acc} \triangleq b^b_{acc} - \hat{b}^{\hat{b}}_{acc}\ \delta b_{ars} \triangleq b^b_{ars} - \hat{b}^{\hat{b}}_{ars} \tag{33}$$
$$\delta u_b \triangleq u(q^{\hat{b}}_b),\ \delta u_a \triangleq u(q^{\hat{a}}_a) \tag{34}$$
$$\delta_\zeta \triangleq \zeta - \hat{\zeta},\ \delta_\xi \triangleq \xi - \hat{\xi} \tag{35}$$

with initial covariance matrices $P_{p,0}$, $P_{v,0}$, $P_{b_{acc},0}$, $P_{u_b,0}$, $P_{b_{ars},0}$, $P_{\zeta,0}$, $P_{\xi,0}$, and $P_{u_a,0}$, respectively. In the following, the error-state kinematics are found. The position error kinematics is found as

$$f_p(t, \hat{x}, \delta x) \triangleq \delta\dot{p} = \delta v \tag{36}$$

The velocity error kinematics is found to be

$$\begin{aligned} f_v(t, \hat{x}, \delta x) \triangleq \delta\dot{v} =& R^n_b(f^b_{nb,m} - b^b_{acc} - \epsilon_{acc}) \\ & - R^n_{\hat{b}}(f^b_{nb,m} - \hat{b}^{\hat{b}}_{acc}) \\ =& R^n_{\hat{b}}R^{\hat{b}}_b(f^b_{nb,m} - \delta b_{acc} - \hat{b}^{\hat{b}}_{acc} - \epsilon_{acc}) \\ & - R^n_{\hat{b}}(f^b_{nb,m} - \hat{b}^{\hat{b}}_{acc}) \\ \approx& R^n_{\hat{b}}S(\delta u_b)(f^b_{nb,m} - \hat{b}^{\hat{b}}_{acc}) \\ & - R^n_{\hat{b}}(I + S(\delta u_b))(\delta b_{acc} + \epsilon_{acc}) \end{aligned} \tag{37}$$

where the small-angle approximation

$$R(u_b) \approx I_3 + S(u_b) \tag{38}$$

is used. The acceleration bias error kinematics is

$$f_{b_{acc}}(t, \hat{x}, \delta x) \triangleq \delta\dot{b}_{acc} = \epsilon_{b_{acc}} \tag{39}$$

The attitude error kinematics can be derived from equation (3.47) in Markley and Crassidis [18]:

$$\delta\dot{u}_b = \omega^b_{nb,m} - b^b_{ars} - R^{\hat{b}\top}_b(\omega^b_{nb,m} - \hat{b}^{\hat{b}}_{ars}) \tag{40}$$

$$f_u(t, \delta x, \hat{x}) \triangleq \delta\dot{u}_b \approx -\delta b_{ars} - S(\omega^b_{nb,m} - \hat{b}^{\hat{b}}_{ars})\delta u_b \tag{41}$$

The ARS bias error kinematics is

$$f_{b_{ars}}(t, \hat{x}, \delta x) \triangleq \delta\dot{b}_{ars} = \epsilon_{b_{ars}} \tag{42}$$

The lever-arm angles error kinematics is

$$f_\zeta(t, \hat{x}, \delta x) \triangleq \delta\dot{\zeta} = \epsilon_\zeta \tag{43}$$
$$f_\xi(t, \hat{x}, \delta x) \triangleq \delta\dot{\xi} = \epsilon_\xi \tag{44}$$

for one antenna and

$$f_{u_a}(t, \hat{x}, \delta x) \triangleq \delta\dot{u}_a = \epsilon_a \tag{45}$$

for multiple antennas, where $\epsilon_\zeta \sim \mathcal{N}(0, Q_\zeta)$, $\epsilon_\xi \sim \mathcal{N}(0, Q_\xi)$, and $\epsilon_a \sim \mathcal{N}(0, Q_a)$ are noise terms that are added to drive estimation. The error kinematics for multiple antennas is concatenated into

$$f(t, \delta x, \hat{x}) = \begin{bmatrix} f_p(t, \delta x, \hat{x}) \\ f_v(t, \delta x, \hat{x}) \\ f_{b_{acc}}(t, \delta x, \hat{x}) \\ f_{u_b}(t, \delta x, \hat{x}) \\ f_{b_{ars}}(t, \delta x, \hat{x}) \\ f_{u_a}(t, \delta x, \hat{x}) \end{bmatrix} \tag{46}$$

Now we can find the first-order linearized kinematics

$$F(t,\delta x,\hat{x}) = \left.\frac{\mathrm{d}f(t,\delta x,\hat{x})}{\mathrm{d}\delta x}\right|_{\delta x=0} \tag{47}$$
$$= \begin{bmatrix} 0_3 & F_{pv} & 0_3 & 0_3 & 0_3 & 0_3 \\ 0_3 & 0_3 & F_{vb_{acc}} & F_{vu_b} & 0_3 & 0_3 \\ 0_3 & 0_3 & 0_3 & 0_3 & 0_3 & 0_3 \\ 0_3 & 0_3 & 0_3 & F_{u_bu_b} & F_{u_bb_{ars}} & 0_3 \\ 0_3 & 0_3 & 0_3 & 0_3 & 0_3 & 0_3 \\ 0_3 & 0_3 & 0_3 & 0_3 & 0_3 & 0_3 \end{bmatrix}$$

where

$$F_{cd} = \frac{\mathrm{d}f_c(t,\delta x,\hat{x})}{\mathrm{d}\delta d},$$

c and d are placeholder symbols, and

$$F_{pv} = I_3,\ F_{vb_{acc}} = -R^n_{\hat{b}},\ F_{vu_b} = -R^n_{\hat{b}} S(f^b_{nb,m} - \hat{b}^{\hat{b}}_{acc})$$
$$F_{u_bu_b} = -S(\omega^b_{nb,m} - \hat{b}^{\hat{b}}_{ars}),\ F_{u_bb_{ars}} = -I_3$$

For one antenna, f and F are identical except they are one row and one row and column smaller, respectively.

B. Measurement Error Model

For multiple antennas, let the predicted measurement be given by

$$\hat{y}_i = \hat{p}^n_{nb} + R^n_{\hat{b}} R^b_{\hat{a}} p^a_{ba_i} \tag{48}$$

and define $\delta y_i \triangleq y_i - \hat{y}_i$. Now, the model for GNSS measurement errors can be found as

$$\begin{aligned} h_i(t,\delta x,\hat{x}) =& \delta y_i = p^n_{na_i,m} - (\hat{p}^n_{nb} + R^n_{\hat{b}} R^b_{\hat{a}} p^a_{ba_i}) \\ =& p^n_{nb} + R^n_b R^b_a p^a_{ba_i} + \epsilon_{p,i} - (\hat{p}^n_{nb} + R^n_{\hat{b}} R^b_{\hat{a}} p^a_{ba_i}) \\ =& \delta p + (R^n_{\hat{b}} R^{\hat{b}}_b R^b_{\hat{a}} R^{\hat{a}}_a - R^n_{\hat{b}} R^b_{\hat{a}}) p^a_{ba_i} + \epsilon_{p,i} \\ \approx& \delta p - R^n_{\hat{b}} S(R^b_{\hat{a}} p^a_{ba_i}) \delta u_b - R^n_{\hat{b}} R^b_{\hat{a}} S(p^a_{ba_i}) \delta u_a \\ &+ R^n_{\hat{b}} S(\delta u_b) R^b_{\hat{a}} S(\delta u_a) p^a_{ba_i} + \epsilon_{p,i} \end{aligned} \tag{49}$$

where (38) was used and

$$\begin{aligned} R^n_{\hat{b}} R^{\hat{b}}_b R^b_{\hat{a}} R^{\hat{a}}_a \approx& R^n_{\hat{b}} (I + S(\delta u_b)) R^b_{\hat{a}} (I + S(\delta u_a)) \\ =& R^n_{\hat{b}} R^b_{\hat{a}} + R^n_{\hat{b}} S(\delta u_b) R^b_{\hat{a}} \\ &+ R^n_{\hat{b}} R^b_{\hat{a}} S(\delta u_a) + R^n_{\hat{b}} S(\delta u_b) R^b_{\hat{a}} S(\delta u_a) \end{aligned}$$

Now, we can find the measurement matrix as

$$\begin{aligned} H_i &= \left.\frac{\mathrm{d}h_i}{\mathrm{d}\delta x}\right|_{\delta x=0} \\ &= \begin{bmatrix} H_{p,i} & 0_3 & 0_3 & H_{u_b,i} & 0_3 & H_{u_a,i} \end{bmatrix} \end{aligned} \tag{50}$$

where

$$H_{c,i} = \left.\frac{\mathrm{d}h_i(t,\delta x,\hat{x})}{\mathrm{d}\delta c}\right|_{\delta x=0},$$

c is a placeholder symbol, and

$$H_{p,i} = I_3,\ H_{u_b,i} = -R^n_{\hat{b}} S(R^b_{\hat{a}} p^a_{ba_i})$$
$$H_{u_a,i} = -R^n_{\hat{b}} R^b_{\hat{a}} S(p^a_{ba_i})$$

The derivations for one antenna is similar, and it is trivial to find

$$\begin{aligned} H_1 &= \left.\frac{\mathrm{d}h_i}{\mathrm{d}\delta x}\right|_{\delta x=0} \\ &= \begin{bmatrix} H_{p,i} & 0_3 & 0_3 & H_{u_b,i} & 0_3 & H_{\zeta,i} & H_{\xi,i} \end{bmatrix} \end{aligned} \tag{51}$$

where

$$[H_{\zeta,i}, H_{\xi,i}] = L_1 \begin{bmatrix} -\sin(\zeta)\cos(\xi) & -\cos(\zeta)\sin(\xi) \\ -\sin(\zeta)\sin(\xi) & \cos(\zeta)\cos(\xi) \\ -\cos(\zeta) & 0 \end{bmatrix}$$

V. Results

The suggested filter developed in Section IV, denoted EKF1 from now on, is compared with two other filters:

- EKF2: error-state EKF in which each lever arm is represented as a three-parameter position variable. In order to use the information about the known GNSS lever arm distances, they are here used as pseudo-measurements

$$y_{L_i} = L_i + \epsilon_{L_i} \tag{52a}$$
$$y_{L_{ij}} = L_{ij} + \epsilon_{L_{ij}} \tag{52b}$$

  where $\epsilon_{L_i} \sim \mathcal{N}(0, R_{L_i})$ and $\epsilon_{L_i} \sim \mathcal{N}(0, R_{L_{ij}})$ are noise terms. The noise terms are added only to ensure non-singularity of the measurement covariance matrix R and no noise is in practice added to the measurement.
- EKF3: error-state EKF in which the lever arms are exactly known.

As shown by Hong et al. [1, 2, 4] and Lee et al. [3], the estimation of lever arms depend on excitation of the vehicle's angular velocities. Therefore, a persistently excited flight pattern is used, generated by

$$\phi(t) = \frac{\pi}{12}\sin\frac{2\pi t}{15} + \frac{\pi}{10}\sin\frac{2\pi t}{120} \tag{53}$$
$$\theta(t) = \frac{\pi}{9}\sin\frac{2\pi t}{15},\ \dot{\psi}(t) = \frac{\|g^n\|_2}{\|v^n_{nb}\|_2}\phi(t) \tag{54}$$
$$v^b_{nb} = \begin{bmatrix} 30 & 0 & 0 \end{bmatrix}^\top \frac{m}{s} \tag{55}$$

where ϕ, θ, and ψ are the roll, pitch, and yaw angles, respectively. The simulated flight lasts 1800 seconds. 50 simulations are conducted for one, two, and three antennas on board the UAV with different sensor noises and initial errors, all drawn from random processes and different in each simulation.

The accelerometer and ARS biases in the simulations are $b^b_{acc} = [0.1, -0.2, 0.15] m/s^2$ and $b^b_{ars} = [0.08, -0.06, -0.1] rad/s$. The lever arms are $p^b_{ba_1} = [0.5, 0, -0.3] m$, $p^b_{ba_2} = [-0.25, 0.9, -0.2] m$, and $p^b_{ba_3} = [-0.25, -0.9, -0.2]$. The true sensor noises are

$$Q_{acc} = 10^{-6} I_3 \quad Q_{ars} = 10^{-6} I_3 \quad \mathcal{R}_i = 5 \cdot 10^{-4} I_3 \tag{56}$$

The IMU measurements are gathered at 100 Hz while the GNSS measurements are gathered at 1 Hz.

The initial position, velocity, and attitude estimates of the EKFs are drawn from Gaussian processes with standard

deviation of $10m$, $1m/s$, and $0.2rad$, respectively. The initial bias estimates are both drawn from Gaussian processes with standard deviation $5 \cdot 10^{-3} m/s^2$ and $5 \cdot 10^{-3} rad/s$, respectively. The initial lever arm angle estimates in Euler angles is drawn uniformly between 0 and $0.2rad$ for both one and more receivers. EKF2's initial lever arm estimates are found using the initial lever arm angle estimates.

The filters are tuned identically for their common states, but some different tuning are used for single and for multiple antennas. The true measurement error covariances in (56) are used in the filters. The ARS bias error covariance is chosen as $Q_{b_{ars}} = 10^{-8} I_3$, whereas the accelerometer error covariances are chosen as $Q_{b_{acc}} = 10^{-6} I_3$ with one antenna and $Q_{b_{acc}} = 10^{-7} I_3$ for two and three antennas. The error covariances for lever arm angles are $Q_\zeta = Q_\xi = 5 \cdot 10^{-5}$ and $Q_a = 10\theta^{-6}$. The initial covariance estimates are for multiple antennas

$$P_{p,0} = 20 I_3 \qquad P_{v,0} = 2 I_3 \qquad P_{b_{acc},0} = 10^{-3} I_3$$
$$P_{u_b,0} = 0.5 I_3 \quad P_{u_a,0} = 10^{-6} I_3 \quad P_{b_{ars},0} = 10^{-3} I_3$$

The same values are used for one antenna, except $P_{b_{acc},0} = 10^{-4} I_3$, $P_{b_{ars},0} = 10^{-4} I_3$, and $P_{\zeta,0} = P_{\xi,0} = 10^{-3} I_2$.

For EKF2, the model $\dot{p}^b_{ba_i} = \epsilon_{ba,i}$ is used where $\epsilon_{ba,i} \sim (0, Q_{ba,i})$ with the initialization error covariance $P_{ba,i0}$. For one antennas, $Q_{ba,1} = 4L_1^2 Q_\zeta I_3$ and $P_{ba,10} = 4L_1^2 P_{\zeta,0} I_3$ are chosen. For multiple antennas, $Q_{ba,i} = 4L_i^2 Q_a$ and $P_{ba,i0} = 4L_i^2 P_{u_a,0}$. The scaling of L_i^2 accounts for the increase in uncertainty with the length of the lever arm. The measurement noise for each of the pseudo-measurements (52) is chosen as $R_{L_i} = R_{L_{ij}} = 10^{-8}$.

The results of the simulations are collected in Tables I–III. They show the mean absolute errors (MAEs) produced by the filters averaged over the 50 simulations. With one antenna, the filters EKF1, EKF2, and EKF3 failed to converge 8, 12, and 14 times, respectively. Therefore, the results of Table I are averaged over the 32 successful simulations, and the 18 unsuccessful are discarded. The reason for the failure of convergence is assumed to be due to insufficient measurements, unfortunate initialization errors, and tuning that was not conservative enough. With two and three antennas, the three filters converged successfully in all simulations.

Comparing EKF1 and EKF2, we see that EKF2 has a slightly lower transient MAE, while the EKF1 a slightly lower steady state MAE. The differences are small enough to be explained by slight differences in tuning, and the two filters must be said to yield similar performance. This means that the suggested filter yields a lower computational complexity than the straight-forward approach of EKF2 without any loss in performance.

Figure 3 shows the absolute estimation error of the x-axis component of GNSS antenna 1 for one, two, and three antennas, respectively. The y- and z-components display similar behaviors. It confirms that EKF2 converges slightly faster at the expense of steady-state performance. Furthermore, the differences in convergence time for one, two, and three antennas are evident. Clearly, the observability of the lever arms increase with the number of lever arms which has a dramatic effect on the transient behavior.

TABLE I: MAEs with one antenna

	Transient			Steady State		
	EKF1	EKF2	EKF3	EKF1	EKF2	EKF3
North [mm]	237.6	210.9	122.3	16.2	16.3	11.8
East [mm]	234.9	229.1	122.2	17.6	17.4	11.6
Down [mm]	185.9	168.1	96.1	12.7	14.3	7.8
Roll [deg]	2.57	2.69	1.85	0.04	0.04	0.04
Pitch [deg]	2.33	2.33	1.65	0.04	0.04	0.04
Yaw [deg]	12.40	12.94	8.76	0.08	0.08	0.08
$\|p^b_{ba_1}\|$ [mm]	210.5	161.9	-	19.8	21.1	-

TABLE II: MAEs with two antennas

	Transient			Steady State		
	EKF1	EKF2	EKF3	EKF1	EKF2	EKF3
North [mm]	22.1	21.5	13.6	9.2	9.4	8.8
East [mm]	21.9	20.8	12.8	9.2	9.4	8.7
Down [mm]	29.7	27.9	13.6	6.7	7.6	5.1
Roll [deg]	0.43	0.42	0.24	0.03	0.03	0.04
Pitch [deg]	0.18	0.19	0.12	0.04	0.04	0.04
Yaw [deg]	0.42	0.44	0.21	0.10	0.09	0.12
$\|p^b_{ba_1}\|$ [mm]	27.1	24.2	-	5.5	7.2	-
$\|p^b_{ba_2}\|$ [mm]	29.0	27.0	-	5.8	7.7	-

Compared to the EKF3 with perfectly known lever arms, we see that EKF1 and EKF2 have slightly larger position errors with one and two antennas in steady state, and no significant difference with three antennas. No significant difference is noticed in attitude errors for any number of antennas.

VI. Conclusion

The position of GNSS antennas relative to the IMU is difficult to measure with high accuracy. However, the distances from GNSS antennas to the IMU and between GNSS antennas are trivial to measure with high accuracy. In this paper, this distance information was used constructively in a novel lever-arm formulation. For one antenna, the lever-arm was expressed in spherical coordinates, yielding two extra states. For multiple antennas, it was shown that all lever-arms could be represented by three rotations from the body-fixed frame to an antenna coordinate frame, thus yielding only three extra states. It was shown in simulations that novel formulation used in an EKF has similar performance as an EKF expressing all lever arms as three-parameter position vectors, yielding a significantly larger state space dimension.

TABLE III: MAEs with three antennas

	Transient			Steady State		
	EKF1	EKF2	EKF3	EKF1	EKF2	EKF3
North [mm]	11.7	11.4	8.5	7.5	7.5	7.4
East [mm]	10.2	10.0	8.2	7.4	7.4	7.4
Down [mm]	7.0	7.0	5.2	4.4	4.4	4.4
Roll [deg]	0.16	0.14	0.04	0.03	0.03	0.04
Pitch [deg]	0.10	0.09	0.04	0.03	0.03	0.03
Yaw [deg]	0.23	0.21	0.11	0.09	0.09	0.10
$\|p^b_{ba_1}\|$ [mm]	5.1	4.3	-	1.6	2.0	-
$\|p^b_{ba_2}\|$ [mm]	7.0	6.1	-	2.0	2.4	-
$\|p^b_{ba_3}\|$ [mm]	4.7	4.8	-	2.0	2.4	-

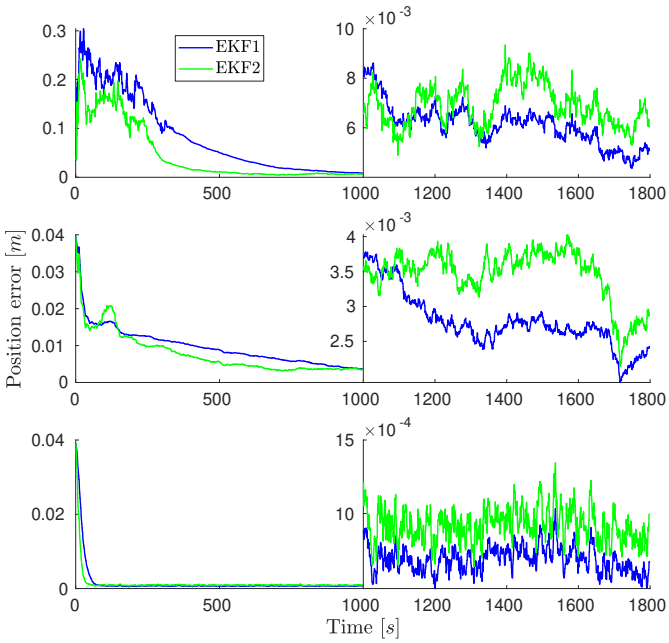

Fig. 3: The absolute estimation error of x-component of GNSS antenna 1 position averaged over all successful simulations for one, two, and three antennas, respectively.

Furthermore, it was shown that the novel EKF performed almost as well as an EKF with perfect knowledge of the lever-arms in the body-fixed frame.

ACKNOWLEDGMENT

This work was supported by the Research Council of Norway (grants no. 261791 and 223254).

REFERENCES

[1] S. Hong et al. "Observability of Error States in GPS/INS Integration". In: *IEEE Transactions on Vehicular Technology* 54.2 (Mar. 2005), pp. 731–743.

[2] S. Hong et al. "Experimental Study on the Estimation of Lever Arm in GPS/INS". In: *Vehicular Technology, IEEE Transactions on* 55 (Apr. 1, 2006), pp. 431–448.

[3] M. K. Lee et al. "Observability Analysis of Alignment Errors in GPS/INS". In: *Journal of Mechanical Science and Technology* 19.6 (June 2005), pp. 1253–1267.

[4] S. Hong et al. "A Car Test for the Estimation of GPS/INS Alignment Errors". In: *IEEE Transactions on Intelligent Transportation Systems* 5.3 (Sept. 2004), pp. 208–218.

[5] J. Seo et al. "Lever Arm Compensation for GPS/INS/Odometer Integrated System". In: *International Journal of Control, Automation, and Systems* 4.2 (2006), pp. 247–254.

[6] M. Zhong et al. "Simultaneous Lever-Arm Compensation and Disturbance Attenuation of POS for a UAV Surveying System". In: *IEEE Transactions on Instrumentation and Measurement* 65.12 (Dec. 2016), pp. 2828–2839.

[7] Q. Cao, M. Zhong, and Y. Zhao. "Dynamic Lever Arm Compensation of SINS/GPS Integrated System for Aerial Mapping". In: *Measurement* 60 (Jan. 2015), pp. 39–49.

[8] K.-W. Chiang et al. "New Calibration Method Using Low Cost MEM IMUs to Verify the Performance of UAV-Borne MMS Payloads". In: *Sensors* 15.3 (Mar. 19, 2015), pp. 6560–6585.

[9] J. Lobo and J. Dias. *Relative Pose Calibration between Visual and Inertial Sensors*. International Journal of Robotics Research, Special Issue 2nd Workshop on Integration of Vision and Inertial Sensors, 26:561–575, 2007. Luiz Gustavo Bizarro, 2009.

[10] N. Montalbano and T. Humphreys. "A Comparison of Methods for Online Lever Arm Estimation in GPS/INS Integration". In: *2018 IEEE/ION Position, Location and Navigation Symposium (PLANS)*. 2018 IEEE/ION Position, Location and Navigation Symposium (PLANS). Apr. 2018, pp. 680–687.

[11] Y. Wu, J. Wang, and D. Hu. "A New Technique for INS/GNSS Attitude and Parameter Estimation Using Online Optimization". In: *IEEE Transactions on Signal Processing* 62.10 (May 2014), pp. 2642–2655.

[12] J. Farrell. *Aided Navigation: GPS with High Rate Sensors*. Electronic engineering. OCLC: ocn212908814. New York: McGraw-Hill, 2008. 530 pp.

[13] M. George and S. Sukkarieh. "Tightly Coupled INS/GPS with Bias Estimation for UAV Applications". In: *Proceedings of the 2005 Australasian Conference on Robotics and Automation, ACRA 2005* (Jan. 1, 2005).

[14] B. Vik and T. I. Fossen. "A Nonlinear Observer for GPS and INS Integration". In: *Proceedings of the 40th IEEE Conference on Decision and Control (Cat. No.01CH37228)*. Proceedings of the 40th IEEE Conference on Decision and Control (Cat. No.01CH37228). Vol. 3. Dec. 2001, 2956–2961 vol.3.

[15] M.-D. Hua. "Attitude Estimation for Accelerated Vehicles Using GPS/INS Measurements". In: *Control Engineering Practice* 18.7 (July 2010), pp. 723–732.

[16] H. F. Grip et al. "Globally Exponentially Stable Attitude and Gyro Bias Estimation with Application to GNSS/INS Integration". In: *Automatica* 51 (Jan. 2015), pp. 158–166.

[17] J. M. Hansen, T. A. Johansen, and T. I. Fossen. "Tightly Coupled Integrated Inertial and Real-Time-Kinematic Positioning Approach Using Nonlinear Observer". In: *2016 American Control Conference (ACC)*. 2016 American Control Conference (ACC). Boston, MA, USA: IEEE, July 2016, pp. 5511–5518.

[18] F. L. Markley and J. L. Crassidis. *Fundamentals of Spacecraft Attitude Determination and Control*. Space technology library 33. OCLC: ocn882605422. New York: Springer, 2014. 486 pp.

[19] F. L. Markley. "Attitude Error Representations for Kalman Filtering". In: *Journal of Guidance, Control, and Dynamics* 26.2 (Mar. 1, 2003), pp. 311–317.